Lab on a Chip

Accepted Manuscript

RSC Publishing

www.rsc.org/loc
Registered Charity Number 207890

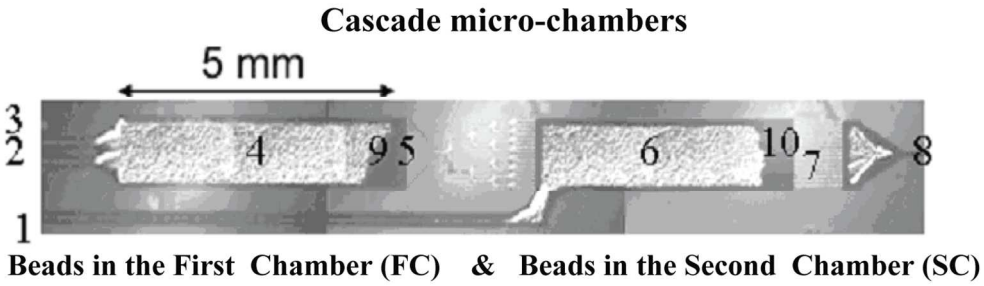

126x35mm (300 x 300 DPI)

Programmable and automated bead-based microfluidics for versatile DNA microarrays under isothermal conditions

Robert Penchovsky*

***To whom the correspondence should be addressed**

Department of Genetics, Faculty of Biology, Sofia University “St. Kliment Ohridski”,
8 Dragan Tzankov Blvd., 1164 Sofia, Bulgaria
E-mail: robert.penchovsky@hotmail.com
Phone/Fax: +35928167340

Abstract

Advances in modern genomic research depend heavily on applications of various devices for automated high- or ultra-throughput arrays. Micro- and nanofluidics offer possibilities for miniaturization and integration of many different arrays onto a single device. Therefore, such devices are becoming a platform of choice for developing analytical instruments for modern biotechnology. This paper presents an implementation of a bead-based microfluidic platform for fully automated and programmable DNA microarrays. The devices are designed to work under isothermal conditions as DNA immobilization and hybridization transfer are performed under steady temperature using reversible pH alterations of reaction solutions. This offers the possibility for integration of more selection modules onto a single chip compared to maintaining a temperature gradient. This novel technology allows integration of many modules on a single reusable chip reducing the application cost. The method takes advantage of demonstrated high-speed DNA hybridization kinetics and denaturation on beads under flow conditions, high-fidelity of DNA hybridization, and small sample volumes needed. The microfluidic devices are applied for a single nucleotide polymorphism analysis and DNA sequencing by synthesis without the need for fluorescent removal step. Apart from that, the microfluidic platform presented is applicable to many areas of modern biotechnology, including biosensor devices, DNA hybridization microarrays, molecular computation, on-chip nucleic acid selection, high-throughput screening of chemical libraries for drug discovery.

Keywords: DNA hybridization under flow conditions, multistep DNA selection, DNA sequencing by synthesis, single nucleotide polymorphism arrays, fluorescence DNA detection

Introduction

In recent years, microfluidic technology has been improving rapidly using the expertise accumulated in the etching of tiny patterns during the mass production of electronic chips. Many methods based on microfluidics have been developed in numerous laboratories for various useful applications[1]. Such applications include parallel gene synthesis[2], on-chip PCR[3, 4], DNA purification[5], separation[6], sequencing[7-9], DNA sizing by single molecule detection[10], DNA hybridization chip arrays[11]. Moreover, microfluidic devices are used for drug discovery[12], pathogen identification[13], cellular analysis[14], bhoghseiochemical clinical assays[15, 16], protein arrays[17] and biosensors[18, 19]. Apart from the high-throughput features[12], microfluidics offer other important advantages such as nanoliter reagent volumes, multi-step processing and on-board mixing of reagents, high reaction rates under flow conditions[20, 21], and possibility for large-scale integration and automation[22-24]. The efforts to construct a lab-on-chip are based on the idea of integration and automation of several chemical procedures, all requiring different reaction conditions, on a single wafer. In practice, owing to the limitations imposed by the enzymatic procedures, and the detection platforms[25], it is difficult to develop compact devices meeting all these criteria.

Despite the significant progress achieved in utilizing the potential of microfluidics for biochemical microarrays[1], what has been lacking is a uniform microfluidic platform for fully automated and integrated processing. Such devices should work in a parallel fashion and should be reusable and therefore, affordable. To be as cheap as possible the device should be based on simple chemical procedures for DNA immobilization, selection, and synthesis.

In this publication, the general idea of multistep sequence-specific nucleic acid selection is implemented on beads-based microfluidics that are fully programmable, automated, and reusable. The selection scheme can be designed to work in parallel, taking into account previous work of developing microfluidic devices for an isothermal DNA selection[26-29].The approach for an isothermal DNA hybridization transfer is based on pH-reversible chemistry for multiple DNA hybridization transfer between cascade microchambers. In addition, a novel general procedure for programmable synthetic DNA immobilization in cascade microchambers is established. A highly

sensitive fluorescence detection system is employed for real-time quantification of DNA hybridization in the microflow reactors.

The approaches, as a whole, take advantage of the fast oligonucleotide hybridization kinetics and denaturation under flow conditions, and the small reagent volumes needed. The microfluidic design takes advantages of the integrated chemical procedures for immobilization and selection. This offers very good opportunities for inexpensive customization not only for DNA chip microarrays. Moreover, it is demonstrated a novel approach for DNA sequencing by synthesis (SBS) that avoids the need for a fluorescent dye removal step. In addition, we demonstrate an automated detection of single nucleotide polymorphism (SNP) in our microfluidic device.

Materials and Methods

Oligonucleotides and beads. The deoxyoligonucleotides used were obtained either from IBA-NAPS (Gottingen, Germany) or from Integrated DNA Technology (Belgium). All of them were purified to HPLC grade. Carboxyl-coated polystyrene super-paramagnetic beads (diameter = 15μm±2μm, with a 15% magnetic content) were purchased from Micromod (Rostock, Germany). Carboxyl-coated PVA beads (diameter = 12μm±3μm, with a 50% magnetic content) were purchased from Chemagen (Baesweiler, Germany). The beads were essentially monodisperse.

Microflow reactors used. The microflow reactors were photolithographically etched onto 100 mm silicon wafers using TMAH (tetramethylammonium hydroxide) and KOH at 80^{o}C. The etched microreactors were sealed with anodically bonded 500μm thick pyrex (borosilicate) glass wafers. Ultrasonically drilled holes in the pyrex wafers (distance between the holes 3.5 mm) allowed the connection of capillary tubing (0.8 mm diameter) using UV-hardening glues to connect the microreactor channels with external fluids.

DNA hybridization transfer in cascade microchambers.

1. Hybridization of perfectly matching DNA (500 nM)to beads in both chambers: The hybridizing buffer (500 mM Tris, pH 8.3, and 50 mM NaCl) containing the DNA7 was

pumped in parallel (4 µl/min) into all three inlets 1, 2 and 3 of the microreactor (**Fig. 2b**).

2. Washing of the beads in both chambers: The beads in both chambers were washed (500 mM Tris, pH 8.3, and 50 mM NaCl without DNA), using inlets 1, 2 and 3 with a flow rate of 4 µl/min. (**Fig. 2b**).

3. Releasing DNA from the beads in the second downstream chamber and washing of the beads in the first chamber: 100 mM NaOH solution was pumped through inlet 1 with a flow rate of 0.01 µl/min and 100 mM Tris, pH 8.3, through inlets 2 and 3 with a flow rate of 0.005 µl/min (**Fig. 2c**).

4. Simultaneous release of DNA from the beads in the first chamber and recovery of the same DNA in the second chamber: A buffering solution of 1 M Tris, pH 8.3, was pumped into the second chamber (inlet 1) with flow rates of 0.01 µl/min and 100 mM NaOH was delivered into the first chamber (inlets 2 and 3) with flow rates of 0.005 µl/min (**Fig. 2d**).

DNA ligation on beads in cascade microchambers. Pfu DNA ligase was purchased from Agilent Technologies, Santa Clara CA. The DNA ligation reactions were performed at 50^{o}C for 5 min in the buffer supplied by the manufacturer. The DNA on the beads was extended by a reverse transcriptase (RT) SuperScript II from Invitrogen, Carlsbad, CA. The reaction was carried out at 42^{o}C for 10 min as described by the manufacturer in the presence of dNTPs purchased from Fermentas, Vilnius, Lithuania. Disulfide linker cyanine 5 (Cy5) labeled nucleotides were purchased from Perkin Elmer, Wellesley, MA and HPLC purified prior to use.

DNA sequencing by synthesis in cascade microchambers. The polymerase synthesis reactions were carried out at 37^{o}C for 3 min using DNA polymerase, one of the four nucleotides (dNTPs) or Cy5-labeled NTPs and all necessary co-factors according to the instructions from Helicos BioSciences.

Fluorescence imaging setup. Fluorescence imaging of DNA/DNA hybridization on beads placed in microreactor chambers was performed using an inverted microscope model Axiovert 100 TV (Carl Zeiss, Jena, Germany). The microscope was connected to an argon-ion laser model 2080-15S (Spectra-Physics Lasers, Inc., CA) by an

optical fiber. A homogeneous pool of light was created by acoustic vibration of the optical fiber at 80 Hz with an arbitrary wave from generator model 3312A (Hewlett-Packard, Palo Alto, CA). The images were detected by 12-bit CCD cameras (models CH250 or Quantix, from Photometrics, Tucson, AZ) connected to the microscope by a C-Mount adapter. An emission filter opening at 540nm and closing at 580nm (Oriel Instruments, Stanford, CT) was employed. The images were obtained and analyzed by the PMIS image processing software (GKR Computer Consulting, Boulder, CO). In all flow experiments, the fluids were delivered to the microreactors by a precision syringe pump model 260 (World Precision Instrument, Sarasota, FL). Constant temperature in the microflow reactors during the experiments was maintained using heating plates connected to a temperature regulator (Philips, Kassel, Germany) and thermometer (Ahlborn, Holzkirchen, Germany).

Results and discussion

A concept of cascade nucleic acid selection (**Fig. 1a**) is implemented on cascade microfluidic chambers (**Fig. 1b**). The input presents an initial pool of DNA oligomers, which undergoes N number selection, synthesis and/or ligation procedures. Molecules from the original pool bind specifically at a definite selection module if they fulfill a certain condition. Otherwise, the molecules are washed out from the microreactor.

All procedures, including bead delivery, DNA immobilization and hybridization transfer, DNA ligation, synthesis and detection are automated. Moreover, both DNA immobilization and hybridization transfer procedures are integrated with the microfluidic design of cascade chambers. Both procedures apply pH-reversible chemistry in which the pH-value of the delivered solutions can be first neutral, after that it can be shifted to high alkaline values (pH ~12) and neutralized again. Therefore, the pH value of the buffering solutions can change several times during the procedures. As a result, we can immobilize any DNA oligomer to the beads placed at any chamber. This makes our microfluidic devices fully programmable.

DNA hybridization kinetics and denaturation on beads under flow conditions.

To establish DNA hybridization transfer under isothermal conditions, we investigated solutions of Hepes, Tris-acetate, and Tris-borate, for their ability to buffer an equal

volume of 100 mM NaOH. In addition, we tested DNA hybridization fidelity in these buffer solutions with DNA hybrids with various mismatches (**Fig. S1**). In these experiments we used carboxytetramethylrhodamine (TAMRA) and QSY7-labeled DNA oligomers. We have used a standard titration curve for quantification of 3'-end TAMRA labeled DNA (**Fig. S2**). We found out that 500 mM Hepes and Tris-acetate buffers, pH 8.3, are suitable for high-fidelity DNA hybridization as well as for buffering an equal volume of 100 mM NaOH with pH change of 0.1 units as detailed in the supplementary section. We chose Tris-acetate buffer for our hybridization experiments since it has less ionic strength than that of Hepes as discussed in the supplementary section.

To test DNA hybridization under flow conditions, carboxyl-coated beads immobilized with DNA1 (**Fig. 1b**) as described in the Supplementary section (**Fig. S5**). A programmable biopolymer immobilization is a very important step in the setup of any biochemical array. A spatially-defined programmable immobilization of DNA oligomers to beads placed in two connected microchambers is demonstrated in **Fig. S5**. The procedure is a combination of three parallel procedures, namely, immobilization by a separate delivery of DNA oligomers and the cross-linking reagent used, pH-dependent inhibition of the immobilization reaction, and immobilization by a reversible pH alteration in cascade microchambers.

The microflow reactor used consists of three inlet channels, a chamber with a bead barrier, and one outlet channel. The etched bead barrier restrained the 12μm super-paramagnetic beads, delivered through the inlet channels, from leaving the bead chamber. The reactor was produced using two masks etched to different depths. The first mask (**Fig. 1b**), forming the bead chamber, was etched to a depth of 10μm. The second mask (**Fig. 1b**), forming the inlet (on the top) and outlet (on the bottom) channels, is etched to a depth of 75μm and to a width of 180μm.

The hybridization experiments were carried out in 500 mM Tris-acetate buffer, pH 8.3, and 50 mM NaCl in the presence of 1 μM and 50 nM 5'-end rhodamine 6G (R6G) labeled DNA oligomers at 45^{o}C. Amino-modified at the 5'-end synthetic DNA1 has immobilized to carboxyl-coated beads (**Fig. 1c**) placed in the microreactor (**Fig. 1b**) as described in the next section.

First, 21 nt, 5'-end R6G labeled, perfectly matching single-stranded DNA2 (**Fig. 1c**), was delivered through all inlets with a flow rate of 10 µl/min. The hybridization reactions in all experiments (**Fig. 1d**) start after the 15th second (s) when the solution with 5'-end R6G-labled DNA enters the chamber with beads (**Fig. 1b**). Fluorescence images from the beads were obtained using CH250 camera with intervals of 2s and exposure of 1s. The results obtained, are plotted in black for 1 µM DNA2 and in yellow for 50 nM in **Fig. 1d**. The average fluorescence signal on the beads reached over 80% saturation for 1 µM DNA2 and 60% saturation for 50 nM DNA2 within 26s and maximum saturation within 100s. The results of similar hybridization experiments are depicted in blue in **Fig. 1d**. The only difference from the previous experiment was the 2000 fold slower flow rate of 0.005 µl/min which doubles the time for reaching over 80% saturation to 50s at 1 µM DNA2. Note that DNA hybridization kinetics under high-flow rate has a nearly exponential curve whereas under low-flow rate has a linear curve.

To prove the specificity of DNA hybridization reaction on beads, 5'-end R6G labeled DNA3, with five mismatches (**Fig. 1c**) was delivered under the same conditions at a flow rate of 10 µl/min. The fluorescence signal on the beads is plotted in red in **Fig. 1d**. It reached about 80% saturation within 20s while that signal was approximately 20% of the hybridization signal for perfectly matching DNA. The small increase of the fluorescence signal on the beads after the 30s may be more a result of a non-specific DNA attachment rather than a DNA/DNA hybridization reaction. After 2 min the hybridization solution was replaced with a washing buffer of 100 mM Tris-acetate pH 8.3 as a fluorescent signal decreased to about 35 arbitrary units (AU). This is only 10 AU above the background signal.

DNA/DNA denaturation on beads under flow conditions was tested using two different concentrations of sodium hydroxide (100 mM and 50 mM). Perfectly matching, 5'-end R6G-labeled DNA2 (**Fig. 1c**) was hybridized to beads placed in a microchamber as described above. Next, the unbound DNA was washed out by delivering a 500 mM Tris-acetate solution for 10 min through all inlet channels, pH 8.3, without DNA. Finally, two different solutions of NaOH (100 mM and 50 mM) were delivered through all inlet channels while the fluorescence images of the beads were taken (see M&M). The average fluorescence signal on the beads is depicted in **Fig.**

1e. The DNA/DNA denaturation on beads using those two different concentrations of sodium hydroxide is an almost instantaneous process taking place within 2s with 100 mM NaOH. The denaturation with 100 mM NaOH seems to be twice as fast as that with 50 mM NaOH (**Fig. 1e**). It should be mentioned herein that a solution of 100 mM NaOH does not influence the fluorescence signal of R6G as demonstrated in **Fig. S3**.

For oligonucleotides up to 1 kb in length, the hybridization reaction in a homogenous mixture is not diffusion-limited. The hybridization reaction is diffusion-limited when one of the complementary strands is immobilized onto a surface. Note that, the DNA/DNA hybridization on beads under flow conditions above certain flow rate, as we demonstrated, is not a diffusion-limited reaction in contrast to the same hybridization under stationary conditions. That may explain the fast hybridization kinetics observed in those and in other similar experiments. It is well known that oligonucleotide hybridization on a surface when one of the complementary DNA strands is attached to a surface is much slower than when both are free in a solution [30].

Efficiency of DNA transfer between cascade microchambers under isothermal conditions. In this section, we investigate the ability to select, transfer and recover DNA between two cascade microchambers (**Fig. 1b**) under isothermal conditions by reversible pH alterations of the solutions used. Both chambers were filled with carboxyl-coated beads immobilized with 5'-end amino-modified DNA6 (**Fig. 2a**). Perfectly matching 5'-end R6G DNA7 oligomers was used (**Fig. 2a**) for hybridization experiments.

The depicted pH values in the microchambers are based on titration as well as mixing experiments (**Fig. 2**). The differences lie in the slower flow rates and DNAs applied and different DNA oligomes optimized in the current experiment. First, we hybridize perfectly matching DNA to beads in both chambers in a solution of 500 mM Tris, pH 8.3, and 50 mM NaCl (**Fig. 2b**). Next, we washed the beads in the first chamber and denatured DNA hybridized to the beads in the second chamber by NaOH (**Fig. 2b**). Finally, we denatured the hybridized DNA in the first chamber and captured it to the beads in the second chamber by pH-reversible chemistry (**Fig. 2d**). The experimental conditions are described in M&M. Note that the amount of beads in

both chambers was equal. The specificity of hybridization transfer with DNA strands with mismatches under the same buffering solutions is demonstrated in **Fig. S5**.

The results are presented in **Fig. 2e**, showing the quantification of DNA on the beads in the two chambers at all stages of the procedure. The DNA transfer yield was calculated as the average fluorescence signal on the beads from the second chamber after the re-hybridization experiment was related to the average fluorescence signal on the beads from the first chamber immediately before the DNA transfer (**Fig. 2e**). The DNA recovery yield was established to be about 67%, which is more than previously observed[28] due to more efficient mixing achieved in the presented experiment (**Fig. S4**). The yield may be increased to 90% and more if there will be an excess of five times of immobilized DNA to the beads in a comparison to the amount of DNA in the free solution. The introduction of a washing step increases the fidelity of the selection procedure. The same procedure can be used for RNA selection. RNAs will be exposed to NaOH for short intervals of time (for seconds) that will not compromise its stability [31]. To further increase RNA stability the Tris-acetate, pH 8.3, buffer can be replaced by a Hepes buffer with pH 7.5. The neutral pH will additionally increase the RNA stability. Note that the DNA hybridization transfer demonstrated herein can be employed for DNA selection in parallel using the microfluidic design depicted in **Fig. S7**.

Automated SNP detection in cascade microchambers. The SNPs are the most abundant variations in the human genome [32]. Various SNPs are associated with genetic disorders in humans. As a result of the advancement of the second generation sequencing machines, more complete sequenced human genomes are becoming available. This increases the chances for the discovery of new SNPs linked with certain diseases in the human population. Therefore, there is a growing demand for the development of straight-forward approaches for SNPs detection. Such approaches should be completely automated and cost efficient to probe as many patients as possible.

Here we present a SNP detection approach based on the DNA hybridization transfer between cascade microchambers described in the previous section. Two different DNA oligomers are attached on beads placed in the first (DNA8) and in the second (DNA9) chambers employing the procedure for programmable DNA immobilization in

cascade microchambers (**Fig. 3a**) as described in a preceding section. Two 16mer DNA oligomers (DNA10 and DNA11) were delivered in both chambers solved in a hybridization buffer (500 mM Tris-acetate, 50 mM NaCl). They are complementary to DNA8 immobilized on the beads in the FC. Next, the beads in the FC were washed with 100 mM Tris-acetate buffer pH 8.3 while the beads in the SC were treated with NaOH. As a result, there was DNA hybridization in the FC only (**Fig. 3b**). The immobilized DNA on the beads can be obtained from a real world sample by a PCR amplification of short (40-50 bp) region of genomic DNA using one 5'-end amino modified primer for immobilizing ssDNA to the beads as shown in Fig.3b.

A image from the SC was taken as the average fluorescence signal (~60 AU) from the beads is depicted in **Fig. 3d**. Note that the DNA11 was R6G-labeled at the 5'-end while the DNA11 has a phosphate at this position. Next, a high-fidelity DNA ligation mixture was pumped for 30 min through inlets 2 and 3 in the FC, while a 100 mM Tris-acetate buffer was delivered via inlet 1 as detailed in M&M. After that, we made a DNA hybridization transfer from the FC to the SC as described in the previous section. A image from the SC was taken as the average fluorescence signal (~1600 AU) from the beads is depicted in **Fig. 3d**. The DNA9 is partially complementary to DNA10 and DNA11. There is a complementary region of 13nt formed after the ligation of DNA10 and DNA11, which form DNA12 (**Fig. 3b**). This can explain the fluorescence signal detected on the beads in the SC.

We carried out the same experiment but with a single nucleotide substitution at the 5'-end of DNA11, where instead of G we had A (DNA13, **Fig. 3c**). After ligation, washing, and DNA hybridization transfer, no fluorescence signal has detected on the beads in the SC (**Fig. 3d**). This can be explained because no ligation reaction occurred between DNA10 and DNA14 due to the single nucleotide substitution.

The experimental results described in this section suggest that we can successfully apply the technology for DNA hybridization transfer between cascade microchambers for automated detection of SNPs. We can do many SNPs detection experiments in parallel using the microfluidics platform (**Fig. S7**) as described in the supplementary section.

Automated DNA sequencing by synthesis in microfluidics without a need for fluorescent dye removal step. The full potential of human genomics will be unleashed only after the complete sequencing of the genomes of many individuals[33]. Therefore advancing of modern sequencing DNA sequencing by synthesis or by ligation (SBL) is used in all second generation sequencing (SGS) machines [34]. These machines have speeded up significantly the sequencing process and have reduced the sequencing cost. As a result, the SGS machines have opened new avenues for novel genomic research with many applications to pharmaceutical industry. However, further cost reduction is needed to make the SGS machines widely used. One of the ways to achieve that is by improving the most inefficient steps of the sequencing process. A fluorescent dye removal step is used in many sequencing machines, including these from 1st and 2nd generation. This step imposes a limitation on the length of the DNA oligonucleotides that are sequenced because it cannot proceed to 100%. As a consequence, the background fluorescence is increasing after each cycle. In addition, the fluorescent removable nucleotide terminators used in SBS or SBL are quite expensive to produce. The alternative approach that avoids fluorescence labeling and therefore, the fluorescent-label removal step, is based on detection of pyrophosphate. Unfortunately, this approach is even more expensive than the fluorescence-based sequencing[35].

Here we present a novel fluorescence-based sequencing method that aims to reduce the sequencing cost by a combination of several basic concepts. They include employing inexpensive fluorescence nucleotides, simplifying the sequencing procedure by excluding the fluorescent dye removal step, and finally, making a re-usable sequencing platform. The successful implementations of these goals result in the development of an efficient DNA sequencing method as described in **Fig. 4**.

Here we present a targeted resequencing approach using primers that define a certain region of interest. This method aims to sequence known regions of interest, focusing on detection of various mutations within them. Isolating such regions of interest through targeted resequencing enables detection of common and rare variants for high-throughput sequencing at a lower cost per sample.

The major costs in DNA sequencing by synthesis come from the expensive nucleotide triphosphates with four different removable fluorescence tags. In addition,

they need four different detection systems. In contrast to many previous approaches, we completely avoid the fluorescent label removal step as shown in **Fig. 4**. Our method reduces the sequencing cost by using inexpensive nucleotide triphosphates labeled with one fluorescence dye and using only one detection system for it. We employ standard Cy5-labeled dNTPs that are quite inexpensive. In fact, such nucleotides were already used in many protocols for RNA and DNA labeling including in DNA SBS [33]. We employ only one type of fluorescence dye. In addition, we use small reaction volumes in our microflow reactors that can be used many times by replacing the beads with new ones. Using the same approach with random primers immobilized on the beads and in the solution we can sequence any unknown DNA sequences Beads are immobilized with a 30mer deoxyribonucleotide (DNA14) placed in both chambers of the cascade microflow reactor (**Fig. 1b**) as described in a preceding section. A template DNA15 that will be sequenced is delivered through the three inlet channels of the microreactor. The template DNA15 and the immobilized DNA14 have an overlapping region of 15 nt at their 3'-ends where they hybridize. Both DNA oligomers were extended by reverse transcriptase at 42^{o}C. “We have used reverse transcriptase to extent our DNA immobilized on the beads to demonstrate the possibility to replace the DNA15 with a RNA template. This will give us the ability to sequence RNA molecules applying the same scheme.

The extended DNA17 was denatured by 100 mM NaOH and washed out from both chambers. Next, a 15 mer DNA18 was delivered in both chambers. It serves as a primer. At this point, four Cy5-dNTPs were consequently, delivered through the SC in the presence of DNA polymerase as described in M&M. Each Cy5-dNTP was pumped over 10 min following by a washing step for 5 min. A fluorescence image from the beads placed in the SC was taken as shown in **Fig. 4b**. A fluorescence signal is observed only in the presence of Cy5-dTTP. Next, the fluorescently labeled DNA18 was denaturized by NaOH and washed out from the SC (**Fig. 4a**). After that, the DNA19 in the FC was extended by one nucleotide by delivering of dTTP and DNA polymerase. The extended DNA19 from the FC was denatured by NaOH and transferred on the beads in the SC by pH neutralization as described in the previous section. With this step, we start a new sequencing cycle (**Fig. 4a**).

We have performed 20 consecutive cycles sequencing 20 nucleotides as shown in **Fig. 4c**. The amount of beads placed in the FC was 5 times bigger than that in the SC. This facilitates the saturation of the beads in the SC where the fluorescence extension is happening and makes possible many consecutive sequencing cycles to be executed. Note that the repeated nucleotides are detected by significant decrease of the fluorescence signal compared with the previous one. This is due to the fact that if there is a repeat of the same nucleotides they tend to quench the fluorescence signal of the terminal Cy5-labeled nucleotide. Such approach was already proven in single DNA sequencing experiments.

We demonstrated an automated DNA sequencing in cascade microchambers that avoids the fluorescent dye removal step and relies on inexpensive chemicals. An additional advantage of our sequencing platform is because the beads can be easily replaced with new ones by employing an external magnetic field and therefore, the microflow reactor can be reused many times. Moreover, we described in the supplementary section how the sequencing method established can be implemented on many cascade microchambers that work in parallel (**Fig. S7**). The method is based on detection of the average fluorescence signal of many beads and thereby, is robust to false positive and false-negative signals, which makes it nearly 100% accurate. Despite the small decrease of the fluorescence signal (~ 2%) after cycle on the beads in the SC, we extrapolate that will be able to carry out at least 40 sequencing cycles without any problem. The use of parallel non-labeled DNA synthesis avoids the need for fluorescent dye removal step, which is very advantageous for the whole sequencing process. It makes it cheaper and more robust to errors to the residual fluorescence.

The automated DNA sequencing method presented in this section combines the application of inexpensive chemicals, simplified sequencing procedure, and reusable devices. The integrated approach presents a significant advance in the development and commercialization of low cost sequencing and can have direct impact in this field.

Conclusion

The experimental results presented in this paper, demonstrate a novel approach for integration of inexpensive DNA immobilization and selection in microfluidic devices under isothermal conditions. The cascade microchamber design allows a programmable DNA immobilization in parallel with the potential application of almost any cross-linking DNA immobilization. The pH-reversible chemistry for multi-step DNA hybridization transfer between cascade microchambers allows a multiple DNA selection and integration of many selection modules on a single wafer. The approach avoids the need for a creation of a temperature gradient that is difficult to achieve in silicon.

The approach takes advantages of the fast DNA hybridization kinetics and denaturation on beads under flow conditions; the high fidelity of hybridization reaction under the established conditions; and from the small sample volumes needed. The use of beads, as a solid support for DNA immobilization and hybridization, offers a high surface/volume ratio and makes the microfluidic chips completely reusable. Uniform microfludic architecture for large-scale integration and automation of DNA microarrays is presented in the supplementary section. The design builds on the demonstrated chemical procedures for reversible pH alterations for DNA hybridization transfer under isothermal conditions and on the programmable DNA immobilization in cascade microchambers. The microfludic design is fully automated and integrates both procedures of programmed immobilization and cascade DNA. All these features are of importance for performing many useful applications. Applying nano instead of microfluidics we can achieve even bigger miniaturization and integration of more chambers on a single chip.

We demonstrate applications of our technology for fully automated SNP detection in cascade microchambers. Moreover, we achieved automated DNA sequencing in chambers without a need for fluorescent dye removal step. The approach has the potential for significantly reducing the sequencing cost. In addition, the approach presented can be employed for inexpensive SNP genotyping [36], nucleic acids-based sensor arrays[37], automated selection of aptamers under isothermal conditions, and an implementation of a dataflow like architecture for computation using DNA libraries [38], and high-throughput screening of chemical libraries for drug discovery [39, 40], cell arrays [41], and molecular biosensoring [42].

Acknowledgments

This work was started at Fraunhofer Gesellschaft, IZB-Schloss Birlinghoven, Sankt Augustin, Germany. We thank Marlies Gohlke for producing the microflow reactors used. The work was also supported in part by a grant DDVU02/5/2010 from the Bulgarian National Science Fund (NSF).

References

1. D. Mark, S. Haeberle, G. Roth, F. von Stetten and R. Zengerle, *Chem Soc Rev*, 2010, **39**, 1153-1182.
2. D. S. Kong, P. A. Carr, L. Chen, S. Zhang and J. M. Jacobson, *Nucleic Acids Res*, 2007, **35**, e61.
3. C. S. Liao, G. B. Lee, H. S. Liu, T. M. Hsieh and C. H. Luo, *Nucleic Acids Res*, 2005, **33**, e156.
4. C. Zhang and D. Xing, *Nucleic Acids Res*, 2007, **35**, 4223-4237.
5. M. A. Witek, S. D. Llopis, A. Wheatley, R. L. McCarley and S. A. Soper, *Nucleic Acids Res*, 2006, **34**, e74.
6. J. Han and H. G. Craighead, *Science*, 2000, **288**, 1026-1029.
7. R. F. Service, *Science*, 1998, **282**, 399-401.
8. E. P. Kartalov and S. R. Quake, *Nucleic Acids Res*, 2004, **32**, 2873-2879.
9. S. Bau, N. Schracke, M. Kranzle, H. Wu, P. F. Stahler, J. D. Hoheisel, M. Beier and D. Summerer, *Anal Bioanal Chem*, 2009, **393**, 171-175.
10. M. Foquet, J. Korlach, W. Zipfel, W. W. Webb and H. G. Craighead, *Anal Chem*, 2002, **74**, 1415-1422.
11. B. J. Cheek, A. B. Steel, M. P. Torres, Y. Y. Yu and H. Yang, *Anal Chem*, 2001, **73**, 5777-5783.
12. S. Einav, D. Gerber, P. D. Bryson, E. H. Sklan, M. Elazar, S. J. Maerkl, J. S. Glenn and S. R. Quake, *Nat Biotechnol*, 2008, **26**, 1019-1027.
13. S. W. Yeung, T. M. Lee, H. Cai and I. M. Hsing, *Nucleic Acids Res*, 2006, **34**, e118.
14. A. Tourovskaia, X. Figueroa-Masot and A. Folch, *Lab Chip*, 2005, **5**, 14-19.
15. V. Srinivasan, V. K. Pamula and R. B. Fair, *Lab Chip*, 2004, **4**, 310-315.
16. S. Moon, H. O. Keles, A. Ozcan, A. Khademhosseini, E. Haeggstrom, D. Kuritzkes and U. Demirci, *Biosens Bioelectron*, 2009, **24**, 3208-3214.
17. Y. N. Yang, H. I. Lin, J. H. Wang, S. C. Shiesh and G. B. Lee, *Biosens Bioelectron*, 2009, **24**, 3091-3096.
18. G. K. Kouassi and J. Irudayaraj, *Anal Chem*, 2006, **78**, 3234-3241.
19. S. Choi and J. Chae, *Biosens Bioelectron*, 2009, **25**, 118-123.
20. Z. H. Fan, S. Mangru, R. Granzow, P. Heaney, W. Ho, Q. Dong and R. Kumar, *Anal Chem*, 1999, **71**, 4851-4859.
21. C. Mikkelsen and H. Bruus, *Lab Chip*, 2005, **5**, 1293-1297.
22. T. Thorsen, S. J. Maerkl and S. R. Quake, *Science*, 2002, **298**, 580-584.
23. J. Melin and S. R. Quake, *Annu Rev Biophys Biomol Struct*, 2007, **36**, 213-231.
24. G. M. Whitesides, *Nature*, 2006, **442**, 368-373.
25. D. Psaltis, S. R. Quake and C. Yang, *Nature*, 2006, **442**, 381-386.
26. R. Penchovsky, E. Birch-Hirschfeld and J. S. McCaskill, *Nucleic Acids Res*, 2000, **28**, E98.
27. J. S. McCaskill, *Biosystems*, 2001, **59**, 125-138.
28. R. Penchovsky and J. S. McCaskill, *Lecture Notes in Computer Science*, 2002, **2340**, 10.
29. J. S. McCaskill, R. Penchovsky, M. Gohlke, J. Ackermann and T. Rucker, *Lecture Notes in Computer Science* 2001, **2054**, 7.
30. P. Schwille, F. Oehlenschlager and N. G. Walter, *Biochemistry*, 1996, **35**, 10182-10193.
31. G. A. Soukup and R. R. Breaker, *RNA*, 1999, **5**, 1308-1325.
32. R. Sachidanandam, D. Weissman, S. C. Schmidt, J. M. Kakol, L. D. Stein, G. Marth, S. Sherry, J. C. Mullikin, B. J. Mortimore, D. L. Willey, S. E. Hunt, C. G. Cole, P. C. Coggill, C. M. Rice, Z. Ning, J. Rogers, D. R. Bentley, P. Y. Kwok, E. R. Mardis, R. T. Yeh, B. Schultz, L. Cook, R. Davenport, M. Dante, L. Fulton, L. Hillier, R. H. Waterston, J. D. McPherson, B. Gilman, S. Schaffner, W. J. Van Etten, D. Reich, J. Higgins, M. J. Daly, B. Blumenstiel, J. Baldwin, N. Stange-Thomann, M. C. Zody, L. Linton, E. S. Lander and D. Altshuler, *Nature*, 2001, **409**, 928-933.
33. T. D. Harris, P. R. Buzby, H. Babcock, E. Beer, J. Bowers, I. Braslavsky, M. Causey, J. Colonell, J. Dimeo, J. W. Efcavitch, E. Giladi, J. Gill, J. Healy, M. Jarosz, D. Lapen, K. Moulton, S. R. Quake,

K. Steinmann, E. Thayer, A. Tyurina, R. Ward, H. Weiss and Z. Xie, *Science*, 2008, **320**, 106-109.

34. E. R. Mardis, *Annu Rev Genomics Hum Genet*, 2008, **9**, 387-402.
35. C. W. Fuller, L. R. Middendorf, S. A. Benner, G. M. Church, T. Harris, X. Huang, S. B. Jovanovich, J. R. Nelson, J. A. Schloss, D. C. Schwartz and D. V. Vezenov, *Nat Biotechnol*, 2009, **27**, 1013-1023.
36. G. T. Marth, I. Korf, M. D. Yandell, R. T. Yeh, Z. Gu, H. Zakeri, N. O. Stitziel, L. Hillier, P. Y. Kwok and W. R. Gish, *Nat Genet*, 1999, **23**, 452-456.
37. R. Penchovsky and R. R. Breaker, *Nat Biotechnol*, 2005, **23**, 1424-1433.
38. R. Penchovsky and J. Ackermann, *J Comput Biol*, 2003, **10**, 215-229.
39. K. Blount, I. Puskarz, R. Penchovsky and R. Breaker, *RNA Biol*, 2006, **3**, 77-81.
40. R. Penchovsky and C. C. Stoilova, *Expert Opin Drug Discov*, 2012.
41. R. A. Chandra, E. S. Douglas, R. A. Mathies, C. R. Bertozzi and M. B. Francis, *Angew Chem Int Ed Engl*, 2006, **45**, 896-901.
42. R. Penchovsky, *ACS Synthetic Biology*, 2012, **1**, 471-482.

Figure legends

Fig. 1. Microflow reactor used for DNA hybridization on beads placed in cascade microchambers. (**a**) Multi-step DNA selection in cascade modules. The input presents an initial pool of DNA oligomers, which undergoes N number selection processing. Certain molecules from the initial pool bind reversibly to a definite selection module if a certain selection condition is fulfilled. Otherwise, the molecules are taken out of the system. (**b**) Cascading microfluidic chambers. The microflow reactor consists of three inlet channels (1, 2, and 3), the two chambers (4 and 6), each with its own bead barrier (5 and 7), and one outlet channel (8). Beads are placed into the first (9) and second chamber (10). Two masks were used for the production of the microreactor. The first mask is etched to a 10 μm depth while the second mask is etched to a 220 μm depth. (**c**) DNA hybridization kinetics and denaturation on beads under flow conditions. DNA1 (35mer) was immobilized to 15 μm beads placed in the microflow reactor (**Fig. 1b**). Two different 5'-end R6G labeled DNAs are used for hybridization. DNA2 is a perfectly matching oligomer while a DNA3 oligomer has five mismatches. (d) Hybridization kinetics on beads under flow conditions. Complementary 21 nt DNA oligomers, 5'-end R6G-labeled, at concentrations of 1 μM or 50 nM were dissolved in a 500 mM Tris-acetate buffer solution, pH 8.3, and 50 mM NaCl. After the 110 s, the beads were washed with the hybridization solution in the absence of DNA. Perfectly matching DNA2 was delivered at flow rates of 10 μl/min (black) or 0.005 μl/min (blue). DNA3 with five mismatches was delivered at a flow rate of 10 μl/min (red). (e) DNA denaturation on beads. 5'-end R6G-labeled DNA2 was hybridized to perfectly matching DNA1 attached to the beads. The non-hybridized DNA2 from the solution was removed. Two concentrations (100 or 50 mM) of NaOH were used for DNA denaturation.

Fig. 2. DNA hybridization transfer between connected microreactors selection modules under isothermal conditions. (a) DNA6 is immobilized on the beads and DNA7 is in free solution used for hybridization transfer. The common annotations for (b), (c), and (d) are identical with **Fig. 1b**. The depicted pH values in the microchambers are based on titration as well as mixing experiments (**Fig. S4**). The DNA hybridization transfer is demonstrated in the following steps: (**b**) I: Hybridization 5'-end R6G-labeled DNA7 with DNA6 immobilized on the beads in both chambers. II:

Washing the beads in both chambers. (**c**) III: Washing the beads in the first chamber (4) and DNA denaturation on the beads in the second chamber (5). (**d**) IV: DNA denaturation from the beads in the first chamber (4) and recovery of the same DNA on the beads placed in the second chamber (5). The DNA recovery yield is about 67%. The exposure time was one second. (**e**) Quantitative analysis of DNA hybridization transfer from beads in the first chamber (red) to those in the second chamber (black). Average fluorescence intensity (without the bias signal of the camera) from different stage of DNA transfer is plotted.

Fig. 3. Automated SNPs detection in cascade microchambers. (**a**) Image of the microfluidic device used. For the annotations from 1 to 10 - **Fig. 1b**. (**b**) DNA8 is immobilized to the beads placed in the first chamber while DNA9 is attached to the beads in the second chamber using the chemical procedure depicted in **Fig. S5**. Two DNA oligomers (DNA10 & 11, each 16nt long) that are perfectly matching to DNA8 were delivered through inlets (2, 3) while 100 mM NaOH was pumped via inlet 1 for 10 min. DNA10 was R6G labeled at its 5'-end. After washing a step, a DNA ligase was delivered through all channels for 30 min. Finally, the ligated DNA12 was transferred from the first to the second chamber as described in **Fig. 2**. DNA12 hybridized with 13 bases of the DNA9, and, as a result, its fluorescence signal was detected. (**c**) In this ligation reaction, we use DNA13 instead of DNA10. DNA13 has one mismatch at its 5'-end with DNA9. As a result, the ligation reaction cannot be completed. After the transfer of the DNA oligomers from the first into the second chamber, no fluorescence signal was observed from the beads in the second chamber. (**d**) The average fluorescence signals from the bead placed in the second chamber are depicted from the experiments described in the previous two sections.

Fig. 4. Automated DNA sequencing in cascade microchambers without a need for a fluorescent-label removing step. (**a**) Magnetic beads with immobilized DNA14 are incorporated in the first (FC) and in the second chamber (SC) of the microflow reactor shown in **Fig. 1b**. As a first step (1-hybrization), we deliver a DNA15 template that will be sequenced. DNA14 and DNA15 have a complementary region of 15 nt at their 3'-ends. Both DNA strands are extended by reverse transcriptase (2 – extension). The extended DNA17 template is removed from both chambers by a NaOH denaturation (3-denaturation). DNA18 is delivered in both chambers to serve

as a primer (4 - hybridization). In the step, four Cy5-dNTPs are delivered separately in the presence of DNA polymerase only in the SC. As a result, the primer was extended by one Cy5-dT (5 - one nt extension).The extended primer (Cy5-DNA18) from the second chamber was denatured and washed out (6- denaturation). Next, dTTP and DNA polymerase were pumped through the first chamber. As a result, the primer in the FC gets extended by one dT (7 - one nt extension). The extended primer was denatured by NaOH (8 - denaturaton). The pH of the NaOH was neutralized and the extended primer (DNA19) was delivered in both chambers where hybridized to DNA on the beads (9 – hybridization). A new sequencing cycle was started with a separate delivery of four Cy5-dNTPs and DNA polymerase in the SC (10 – one nt extension). Note that the amount of beads placed in the FC was 5 times bigger than that in the SC. (**b**) Fluorescence images of beads placed in the SC during the sequencing step 5 in the presence of different Cy5-dNTPs. One nucleotide extension of the primer occurred only in the presence of Cy5-dTTP. The red line indicates the area of the beads, which average fluorescence was measured. (**c**) The average fluorescence intensity of 80 images from 20 consequent sequencing cycles is depicted.

Penchovsky, R. Programmable and automated bead-based microfluidics for versatile DNA microarrays under isothermal conditions

Figures

Fig. 1

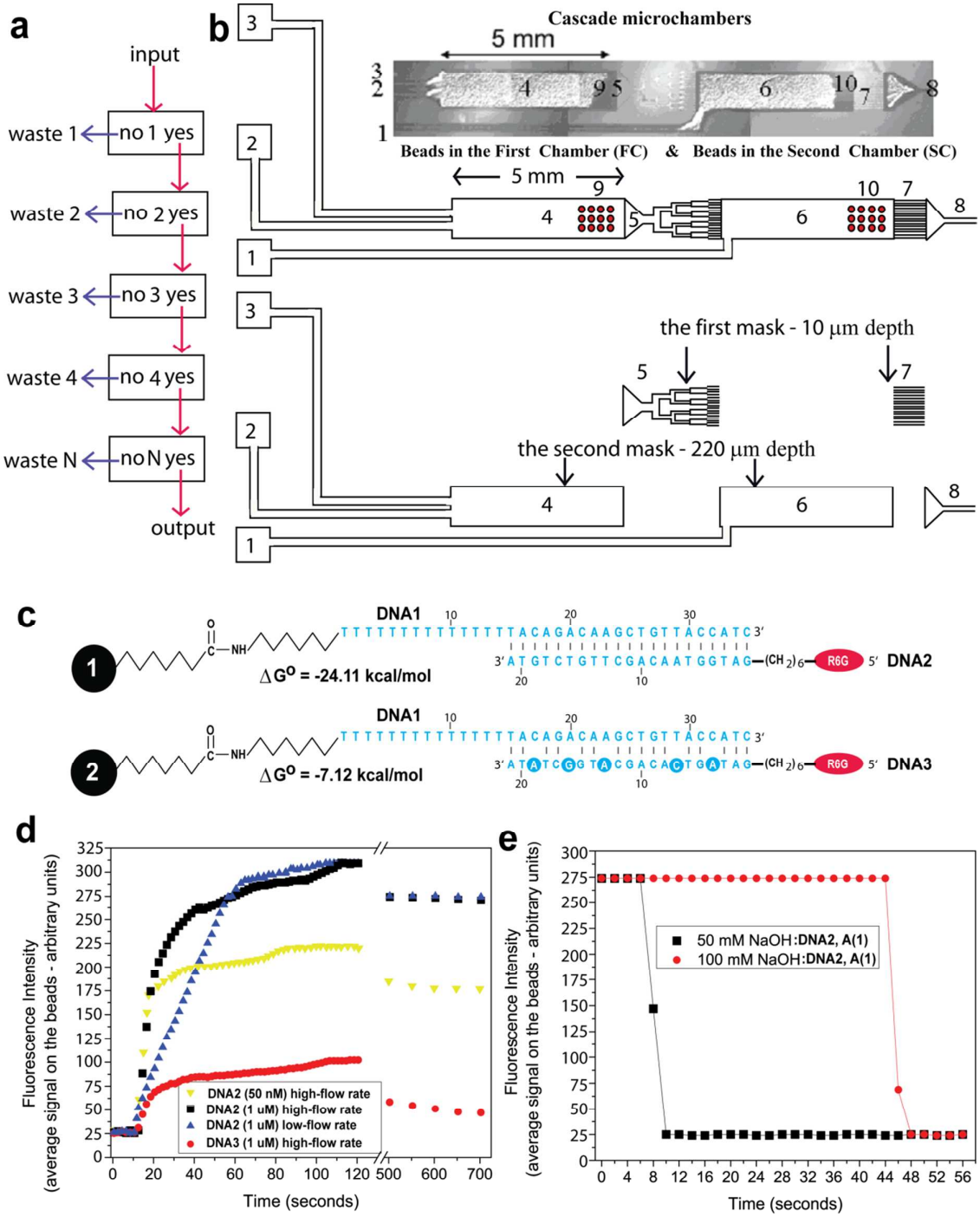

Penchovsky, R. Programmable and automated bead-based microfluidics for versatile DNA microarrays under isothermal conditions

Fig. 2

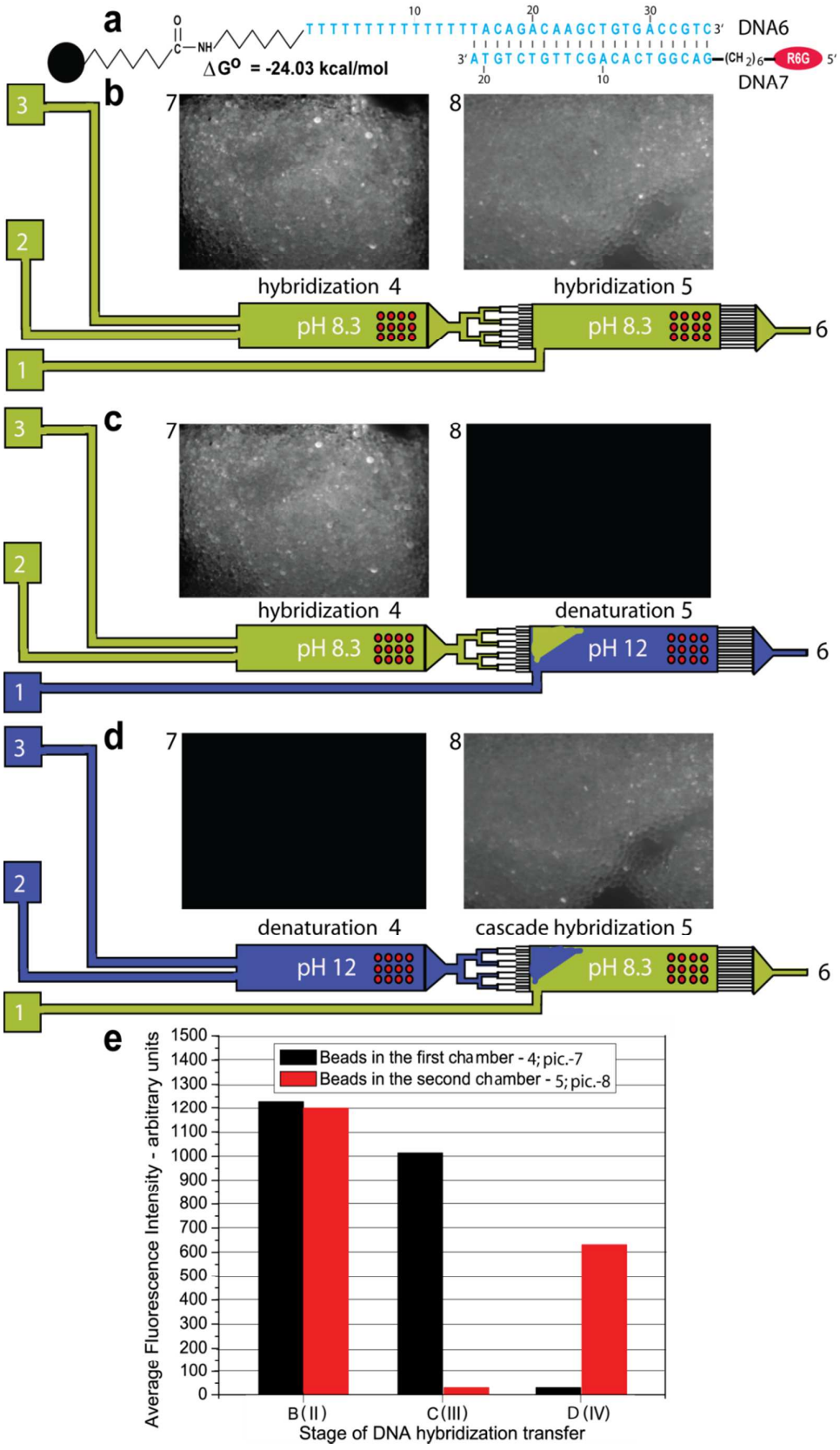

Penchovsky, R. Programmable and automated bead-based microfluidics for versatile DNA microarrays under isothermal conditions

Fig. 3

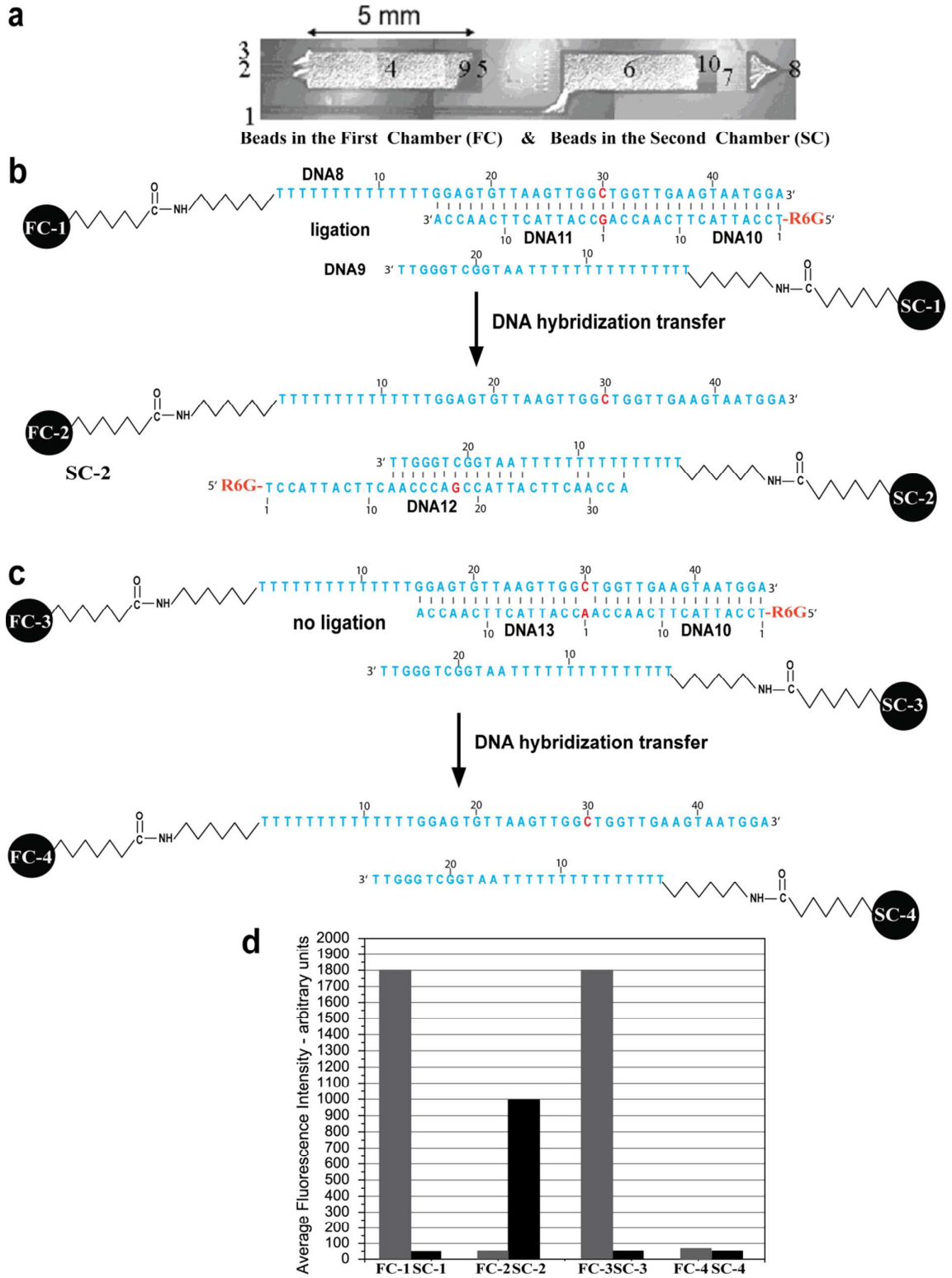

Penchovsky, R. Programmable and automated bead-based microfluidics for versatile DNA microarrays under isothermal conditions

Fig. 4